A giant chlorophyll-protein complex induced by iron deficiency in cyanobacteria

Boekema, E.J.; Hifney, A.; Yakushevska, A.E.; Piotrowski, M.; Keegstra, W.; Berry, S.; Michel, K.-P.; Pistorius, E.K.; Kruip, J.

Published in:
Nature

DOI:
10.1038/35089104

Publication date:
2001

Biochemical characterization

SDS–PAGE and western blotting were performed as described in ref. 18. Optical absorption spectra were measured at room temperature using a Shimadzu MPS 2000 spectrometer. Steady-state fluorescence spectra were obtained using a Perkin Elmer LS50 at 77K and measured with an excitation wavelength of 440 nm. To record excitation spectra, the sample was excited between 650 and 700 nm and the fluorescence detected at 720 nm. HPLC size exclusion analyses were performed using a Phenomenex BioSep SEC S3000 column.

Electron microscopy

Preparations were negatively stained with 2% uranyl acetate on glow discharged carbon evaporated grids, and imaged using a Philips CM 100 electron microscope at 80 kV. The magnification was calibrated to be ×51,500. Twenty electron micrographs were taken for each preparation, and subsequently calculated to have the first minima of contrast transfer function in the range of 17–23 Å.

Image processing and modelling

Electron micrographs were digitized using a Leafscan 45 densitometer set at a step size of 10 μm. Single-particle data sets of approximately 3,000 (CP43′–PSI supercomplex) and 4,000 (PSI trimer) were obtained by interactively selecting all possible particles from the micrographs. All subsequent processing was performed within the IMAGIC-5 software environment[19,20]. The single-particle images were coarsened by a factor of 2 resulting in 3.88 Å per pixel on the specimen scale. Reference free alignment coupled with multivariate statistical classification[21] was used to identify initial class averages, which were then used for iterative refinement until the data merged, resulting in the improved class averages shown.

Co-ordinate data sets were obtained from the RCSB data bank (http://www.rcsb.org) under the entry codes 1C51 (PSI 4 Å structure[10]) and 1FE1 (PSII 3.8 Å structure[11]). These structural models were visualized using the program Swiss-PDB viewer[22] (Glaxo-Wellcome Experimental Research) and overlaid at the same scale onto the calculated single-particle projection maps. The carbon-α backbone for the transmembrane helices of the CP43 subunit was extracted from the 1FE1 co-ordinates and modelled into each subunit of the ring surrounding the PSI trimer, according to the centre of mass observed for each of the 18 subunits within the ring.

Received 16 May; accepted 21 June 2001.

1. Martin, J. H. *et al.* Testing the iron hypothesis in ecosystems of the equatorial Pacific Ocean. *Nature.* **371,** 123–129 (1994).
2. Behrenfeld, M. J., Bale, A. J., Zbigniew, S. K., Aiken, J. & Falkowski, P. G. Confirmation of the iron limitation of phytoplankton photosynthesis in the equatorial Pacific Ocean. *Nature* **383,** 508–511 (1996).
3. Straus, N. A. in *Molecular Biology of Cyanobacteria* (ed. Bryant, D. A.) 731–750 (Kluwer Academic, Dordrecht, 1994).
4. Burnap, R. L., Troyan, T. & Sherman, L. A. The highly abundant chlorophyll-protein complex of iron-deficient *Synechococcus* sp. PCC7942 (CP43′) is encoded by the *isiA* gene. *Plant Physiol.* **103,** 893–902 (1993).
5. Falk, S., Samson, G., Bruce, D., Hunter, N. P. A. & Laudenbach, D. A. Functional analysis of the iron-stress induced CP43′ polypeptide of PSII in the cyanobacterium *Synechococcus* sp. PCC 7942. *Photosynth. Res.* **45,** 51–60 (1995).
6. Park, Y. P. Sandström, S., Gustafsson, P. & Öquist, G. Expression of the *isiA* gene is essential for the survival of the cyanobacterium *Synechococcus* sp. PCC 7942 by protecting photosystem II from excess light under iron limitation. *Mol. Microbiol.* **32,** 123–129 (1999).
7. Bricker, T. M., Morvant, J., Marsi, N., Sutton, H. M. & Frankel, L. K. Isolation of a highly active photosystem II preparation from *Synechocystis* 6803 using a histidine-tagged mutant of CP47. *Biochim. Biophys. Acta.* **1409,** 50–57 (1998).
8. Rögner, M., Mühlenhoff, U., Boekema, E. J. & Witt, H. T. Mono-, di- and trimeric PSI reaction center complexes isolated from the thermophilic cyanobacterium *Synechococcus* sp. Size, shape and activity. *Biochim. Biophys. Acta* **1015,** 415–424 (1989).
9. Boekema, E. J., Boonstra, A. F., Dekker, J. P. & Rögner, M. Electron microscopic structural analysis of photosystem I, photosystem II, and the cytochrome b_6f complex from green plants and cyanobacteria. *J. Bioenerg. Biomembr.* **26,** 17–29 (1994).
10. Krauβ, N. *et al.* Photosystem I at 4 Å resolution represents the first structural model of a joint photosynthetic reaction centre and core antenna system. *Nature Struct. Biol.* **3,** 965–973 (1996).
11. Zouni, A. *et al.* Crystal structure of photosystem II from *Synechococcus elongatus* at 3.8Å resolution. *Nature* **409,** 739–743 (2001).
12. Hankamer, B., Morris, E. P. & Barber, J. Revealing the structure of the oxygen evolving core dimer of photosystem II by cryoelectron crystallography. *Nature Struct. Biol.* **6,** 560–564 (1999).
13. Schubert, W.-D. *et al.* Photosystem I of *Synechococcus elongatus* at 4 Å resolution: Comprehensive structural analysis. *J. Mol. Biol.* **272,** 741–769 (1997).
14. McDermott, G. *et al.* Crystal structure of an integral membrane light-harvesting complex from photosynthetic bacteria. *Nature* **374,** 517–521 (1995).
15. Cogdell, R. J. *et al.* How photosynthetic bacteria harvest solar energy. *J. Bacteriol.* **181,** 3869–3879 (1999).
16. Williams, J. G. K. Construction of specific mutants in PSII photosynthetic reaction centres by genetic engineering methods in *Synechocystis* 6803. *Methods Enzymol.* **167,** 766–778 (1988).
17. Tang, X.-S. & Diner, B. A. Biochemical and spectroscopic characterisation of a new oxygen-evolving photosystem II core complex from the cyanobacterium *Synechocystis* PCC 6803. *Biochemistry* **33,** 4594–4603 (1994).
18. Hankamer, B. *et al.* Isolation and biochemical characterisation of monomeric and dimeric photosystem II complexes from spinach and their relevance to the organisation of photosystem II *in vivo*. *Eur. J. Biochem.* **243,** 422–429 (1997).
19. van Heel, M., Harauz, G. & Orlova, E. V. A new generation of the IMAGIC image processing system. *J. Struct. Biol.* **116,** 17–24 (1996).
20. van Heel, M. *et al.* Single-particle electron cryo-microscopy: towards atomic resolution. *Q. Rev. Biophys.* **33,** 307–369 (2000).
21. Sherman, M., Soejima, T., Chui, W. & van Heel, M. Multi-variate analysis of single unit cells in electron crystallography. *Ultramicroscopy* **74,** 179–199 (1998).
22. Guex, N. & Peitsch, M. C. SWISS-MODEL and the Swiss-Pdb Viewer: An environment for comparative protein modeling. *Electrophoresis* **18,** 2714–2723 (1997).

Acknowledgements

We thank A. Telfer, B. Hankamer, E. Morris, C. Büchel, J. Duncan and P. Da Fonseca for discussions; T. Bricker for supplying the His-tagged *Synechocystis* PCC 6803 mutant; and L. Sherman for supplying the CP43′ antibody. This work was supported by the Biotechnology and Biological Research Council.

Correspondence and requests for materials should be addressed to J.B. (email: j.barber@ic.ac.uk).

A giant chlorophyll–protein complex induced by iron deficiency in cyanobacteria

E. J. Boekema*, A. Hifney†, A. E. Yakushevska*, M. Piotrowski‡, W. Keegstra*, S. Berry§, K.-P. Michel†, E. K. Pistorius† & J. Kruip§

* *Groningen Biomolecular Sciences and Biotechnology Institute, University of Groningen, Nijenborgh 4, 9747 AG Groningen, The Netherlands*
† *Biologie VIII: Zellphysiologie, Universität Bielefeld, D-33501, Bielefeld, Germany*
‡ *Plant Physiology, Ruhr-University Bochum, D-44780 Bochum, Germany*
§ *Plant Biochemistry, Ruhr-University Bochum, D-44780 Bochum, Germany*

Cyanobacteria are abundant throughout most of the world's water bodies and contribute significantly to global primary productivity through oxygenic photosynthesis. This reaction is catalysed by two membrane-bound protein complexes, photosystem I (PSI) and photosystem II (PSII), which both contain chlorophyll-binding subunits functioning as an internal antenna[1]. In addition, phycobilisomes act as peripheral antenna systems, but no additional light-harvesting systems have been found under normal growth conditions. Iron deficiency, which is often the limiting factor for cyanobacterial growth in aquatic ecosystems[2], leads to the induction of additional proteins such as IsiA (ref. 3). Although IsiA has been implicated in chlorophyll storage, energy absorption and protection against excessive light, its precise molecular function and association to other proteins is unknown. Here we report the purification of a specific PSI–IsiA supercomplex, which is abundant under conditions of iron limitation. Electron microscopy shows that this supercomplex consists of trimeric PSI surrounded by a closed ring of 18 IsiA proteins binding around 180 chlorophyll molecules. We provide a structural characterization of an additional chlorophyll-containing, membrane-integral antenna in a cyanobacterial photosystem.

We examined the protein composition of thylakoid membranes from the mesophilic cyanobacterium *Synechococcus* sp. PCC 7942 when cells were grown under conditions of iron limitation. Iron deficiency leads to fast degradation of phycobilisomes[4] and to the expression of iron-regulated genes that enable cells to continue growth[5]. We found a distinct new protein complex in elution profiles of solubilized membrane protein complexes from iron-deficient cells (Fig. 1a). At the same time the amount of trimeric PSI, the most abundant protein complex under normal growth conditions, was reduced by 60–80%. The abundance of the new complex was inversely related to the disappearance of trimeric PSI

and represents an example of membrane-protein dynamics. We purified this complex to homogeneity by using an additional perfusion chromatography step (data not shown). The purified complex had an absorption maximum at 675 nm, resembling PSII (674 nm) rather than PSI (679 nm). Size-exclusion chromatography gave an apparent relative molecular mass of 1,700,000 (M_r 1,700K) for this complex (Fig. 1b). This is much larger than the molecular mass of 900K found for trimeric PSI. Analysis of subunit composition of the new complex by SDS–polyacrylamide gel electrophoresis (PAGE) showed that all major PSI subunits were present (Fig. 1c); however, the complex showed additional protein bands with apparent masses of 36, 48 and 53K (depending on the preparation). Obviously, the complex contains several copies of IsiA that are not always completely denatured and are separated by SDS–PAGE as several bands at higher molecular masses. *De novo* sequencing of tryptic peptides obtained from these bands resulted in perfect matches with the IsiA protein of *Synechococcus* sp. PCC 7942.

IsiA was first identified as a principal protein expressed under iron deficiency[6] and is co-transcribed with flavodoxin, an alternative electron acceptor of PSI (ref. 7). The sequence of IsiA shows strong homologies to the CP43 subunit of PSII. The main difference is the lack of a large hydrophilic loop of about 100 amino acids. The structure of CP43 has been determined to 3.8 Å resolution as part of the dimeric cyanobacterial PSII core complex[8]. CP43 consists of six membrane-spanning α-helices to which at least 12 chlorophyll *a* molecules are bound[8]. As the chlorophyll-binding sites are conserved, a similar chlorophyll content of 12 can be estimated for IsiA. If one assumes an antenna with a chlorophyll content of 96 for PSI, a theoretical antenna size of 168 chlorophyll/P700 is reached for the PSI–IsiA complex (see below for the number of IsiA proteins per PSI). This fits our chlorophyll/P700 measurements, which indicate a 60% increase in antenna size for the PSI–IsiA complex (161 ± 20 chlorophyll/P700) compared with trimeric PSI (103 ± 9 chlorophyll/P700). It was widely assumed that IsiA would interact with PSII (ref. 9) owing to its sequence homologies with CP43. IsiA (also called CP43′) was proposed to protect PSII against excess light[10], function as an alternative antenna for PSII (ref. 9), or act as a chlorophyll-storage protein[5]. In contrast, our data show that IsiA interacts with PSI. Qualitatively, the light-saturation curves of PSI and the PSI–IsiA complex look similar (Fig. 2), but a quantitative analysis using the equation:

$$\Delta A = \Delta A_{max} \times [1 - \exp(-k \times \text{relative flash intensity})] \quad (1)$$

reveals that the absorption cross-section of the PSI–IsiA complex is about 44% higher than for PSI: k, which is a measure of the efficiency of photon capture, is 0.045 ± 0.003 for PSI and 0.065 ± 0.007 for the PSI–IsiA complex; A is the absorbance. This indicates, together with fluorescence spectra and PSI kinetics (data not shown), that IsiA is indeed a functional antenna for PSI. Furthermore, the determined structure of trimeric PSI at 2.5 Å resolution shows chlorophyll molecules that are bound to the outside of PSI (ref. 11). These pigments are ideally positioned for excitation energy transfer from the IsiA ring to the PSI reaction centre.

Imaging of the purified PSI–IsiA complex by electron microscopy revealed large numbers of a circular flat particle with a diameter of 345 Å (Fig. 3a). A data set of top-view projections was analysed by single-particle analysis, which revealed that the new complex is composed of a central trimeric PSI complex surrounded by a ring of 18 densities. Classification of projections indicated that the main variation in the data set was the amount of tilting. Well preserved, three-fold rotational symmetry, which is to be expected from zero-tilted particles, was only present in limited numbers of projections (Fig. 3b), indicating that about 95% of the particles are slightly tilted (Fig. 3c, d). The resolution in the images of Fig. 3b–d is about 22, 14 and 15 Å, respectively, allowing a close interpretation of the projected structure.

First, comparison with previously studied PSI particles indicated that the PSI–IsiA complexes[12,13] are attached to the carbon support film by the bulky stromal surface. Apparently this 40-Å-high stromal ridge and the rather flat ring of peripheral IsiA subunits together cause the slight tilt of most of the particles.

Second, the peripheral IsiA ring can be further interpreted by

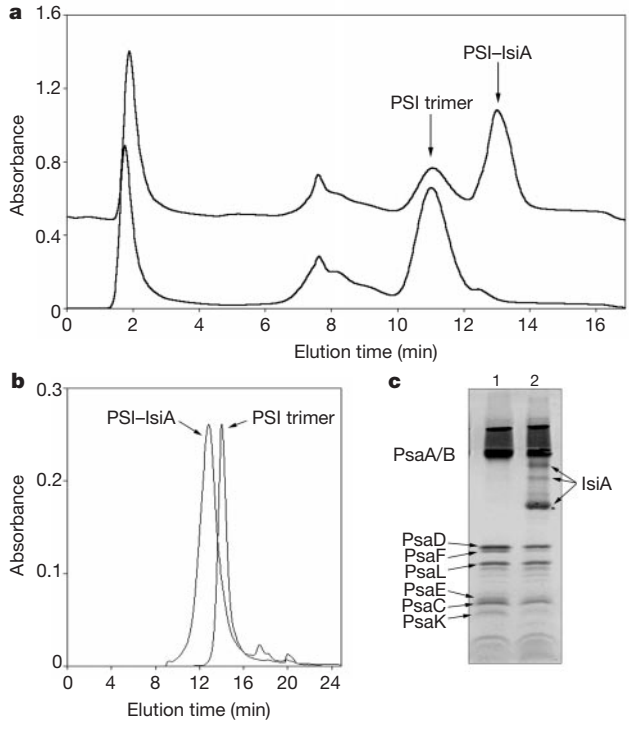

Figure 1 Purification and subunit analysis of the PSI–IsiA complex. **a**, Elution profiles for thylakoid membrane protein extracts of cells grown under either normal (lower trace) or iron-deficient conditions (upper trace). Purification was carried out on an anion-exchange column using a linear magnesium sulphate gradient for elution, and monitored at 435 nm. **b**, Size-exclusion chromatography of purified trimeric PSI and of PSI–IsiA complexes as indicated. **c**, SDS–PAGE and Coomassie staining of trimeric PSI (lane 1) and the PSI–IsiA complex (lane 2). Protein bands other than PSI subunits were assigned by *de novo* sequencing.

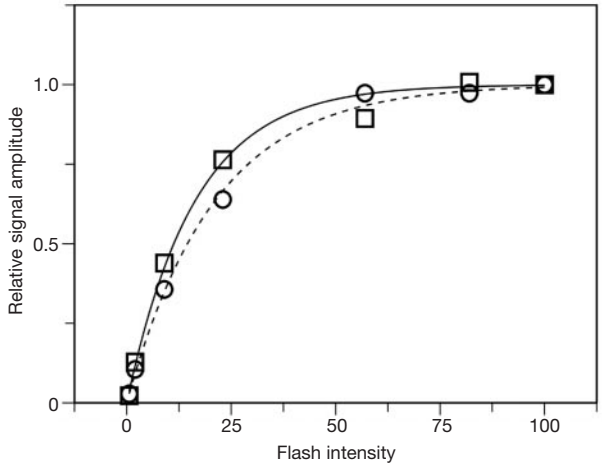

Figure 2 Light-saturation curves of the absorbance changes of PSI (circles and dashed line) and the PSI–IsiA complex (squares and solid line). Flash intensity was varied by a set of neutral-density filters. The absolute values of the signals at 100% flash intensity are $\Delta A = (2.5 \pm 0.2) \times 10^{-3}$ ($n = 7$) for PSI and $\Delta A = (1.6 \pm 0.2) \times 10^{-3}$ ($n = 6$) for PSI–IsiA. The curves are based on equation (1).

comparison to the homologous CP43 subunit of PSII (ref. 8). Its projected density has been modelled into the untilted projection (Fig. 3e) and fits into each of the 18 peripheral densities if the periphery is corrected for an attached detergent shell[14]. From this fit, it can be concluded that the new complex is composed of a ring of 18 IsiA proteins with a diameter of 310 Å. The PSI trimer is not a perfect circle and hence the 18 IsiA proteins do not form a perfect ring either. The two IsiA molecules that bind closest to the centre of each PSI monomer are shifted in an outward direction by about 7 Å and thus have a wider separation.

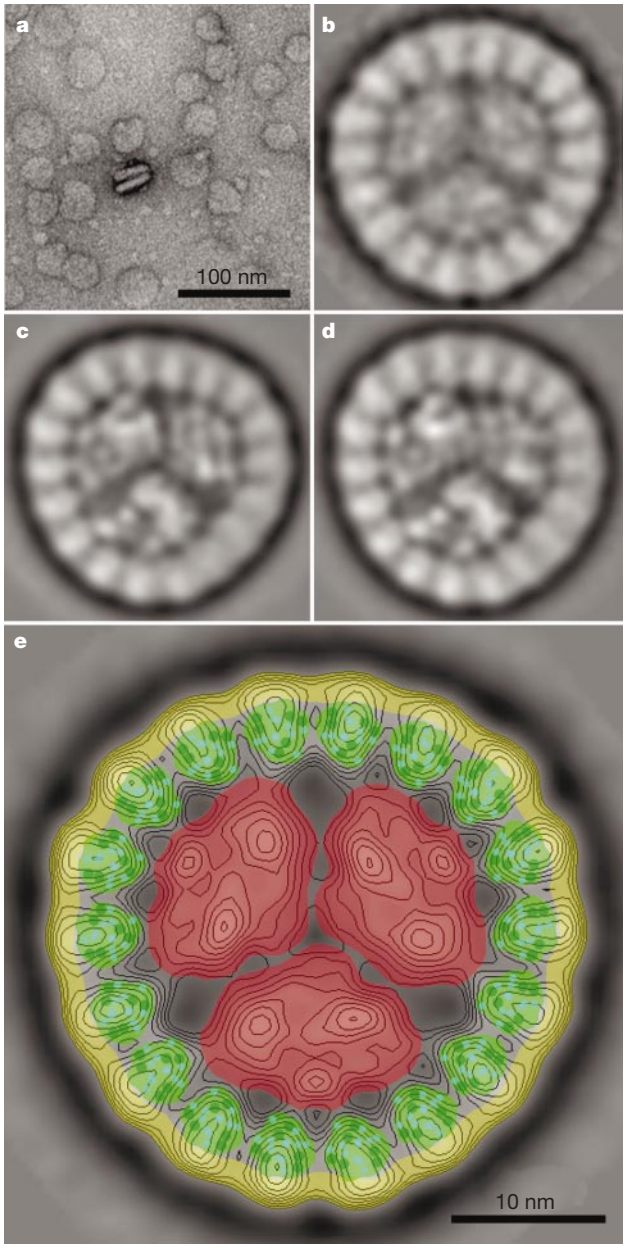

Figure 3 Electron microscopy of PSI–IsiA complexes and their interpretation. **a**, Electron micrograph of isolated complexes, negatively stained with uranyl acetate. **b**–**d**, Results of multivariate statistical analysis and classification of top-view projections; average images of 231 (**b**), 2,000 (**c**) and 2,000 (**d**) projections. **e**, Contoured version of the three-fold-symmetrical class sum from **b**. The centre of the complex is formed by a trimeric PSI complex (red) and is surrounded by a ring of 18 IsiA proteins (green), each consisting of six membrane-spanning α-helices (dark green dots) and 12 chlorophyll *a* molecules (blue dots). A detergent shell (yellow) surrounds the complex in projection. The images are presented as facing from the *p*-side of the thylakoid membrane, which is equivalent to the lumenal side in green plants.

The gene coding for IsiA can be found in various cyanobacterial species where it is present in a single copy. Prochlorophytes, oxygenic prokaryotes possessing chlorophyll *b*, contain so-called *pcb* genes, which bind chlorophyll *b* and resemble IsiA (ref. 15). It will be interesting to discover how light-harvesting complexes are organized in this class of cyanobacteria, especially as it has been shown that prochlorophytes that are adapted to low light conditions contain several variations of *pcb* genes[16]. Our data give a clear structural characterization of a photosystem complex from a cyanobacterium with a peripheral membrane-bound antenna. This PSI–IsiA supercomplex is markedly different from all peripheral membrane-bound antenna complexes observed in green plants, including PSI and PSII (refs 12, 17). The IsiA ring resembles multimers of light-harvesting proteins (LH1 and LH2) found in anoxygenic purple bacteria[18,19]. We now know of three peripheral chlorophyll-binding antenna systems: LH rings in purple bacteria, IsiA rings in cyanobacteria and LHC trimers/dimers in chloroplasts. Despite similarities in organization, all are structurally different from each other and are examples of convergent evolution. □

Methods

Cell culture

Synechococcus sp. PCC 7942 cells were grown in liquid BG-11 medium. Iron deficiency was achieved by omitting iron sources in the medium; cells were grown for 4 days (once diluted) in this medium. Growth conditions were as described[20] except that cultures were illuminated in constant light with fluorescent light tubes (Sylvana Luxline ES 18 W) at a light intensity of 120 $\mu E\, m^{-2}\, s^{-1}$.

PSI–IsiA purification

We isolated the PSI–IsiA complex from *Synechococcus* as described[21] with some modifications. Solubilized membrane protein complexes were purified by anion-exchange chromatography (Poros 50 HQ, Applied Biosystems) using a magnesium sulphate gradient, followed by hydrophobic-interaction chromatography (Poros Butyl, Applied Biosystems) using an ammonium sulphate gradient. We used size-exclusion chromatography (BioSilect 400, Bio-Rad) as a final purification step before electron microscopy. Purified particles were concentrated by ultrafiltration (100K cut-off filter) and stored in buffer containing 20 mM MES, pH 6.5, 10 mM $CaCl_2$, 10 mM $MgCl_2$ and 0.03% β-dodecyl maltoside at −70 °C before use.

Mass spectrometry

Proteins were digested in gel using trypsin (Promega). Peptides were purified and concentrated using ZipTips C18 (Millipore). *De novo* sequencing was done on a quadrupole/time-of-flight hybrid mass spectrometer (Q-TOF2, Micromass) in positive-ion mode.

Electron microscopy

Transmission electron microscopy was performed with a Philips CM10 electron microscope at ×52,000 magnification. We prepared negatively stained specimens on glow-discharged carbon-coated grids. From 119 digitized electron micrographs, 5,200 well preserved top-view projections were extracted for single-particle image analysis. Multi-reference alignment, multivariate statistical analysis and classification were performed with IMAGIC software[22,23] and Grip software.

Difference spectroscopy

Flash-induced absorption changes at 703 nm were measured at a chlorophyll *a* concentration of 4 μM in a buffer containing 50 mM ACES, pH 6.5, 50 mM KCl, 30 μM phenazine methosulphate and 5 mM sodium ascorbate. Saturating blue light flashes were obtained by a xenon flash lamp equipped with blue glass filters. The antenna size was calculated from the signal amplitude using an extinction coefficient of 64 $mM^{-1}\, cm^{-1}$ (ref. 24).

Received 6 June; accepted 29 June 2001.

1. Nitschke, W. & Rutherford, A. Photosynthetic reaction centres: variations on a common structural theme? *Trends Biochem. Sci.* **16,** 241–245 (1991).
2. Behrenfeld, M., Bale, A., Kolber, Z., Aiken, J. & Falkowski, P. Confirmation of iron limitation of phytoplankton photosynthesis in the equatorial pacific ocean. *Nature* **383,** 508–511 (1996).
3. Straus, N. A. (ed.) in *Advances in Photosynthesis* Vol. 1 *The Molecular Biology of Cyanobacteria* (ed. Bryant, D. A.) 731–750 (Kluwer, Dordrecht, 1994).
4. Guikema, J. & Sherman, L. A. Organization and function of chl in membranes of cyanobacteria during iron starvation. *Plant Physiol.* **73,** 250–256 (1983).
5. Burnap, R., Troyan, T. & Sherman, L. A. The highly abundant chlorophyll-protein complex of iron-deficient *Synechococcus* sp. PCC7942 (CP43′) is encoded by the IsiA gene. *Plant Physiol.* **103,** 893–902 (1993).
6. Laudenbach, D. & Straus, N. A. Characterization of a cyanobacterial iron stress-induced gene similar to *psbC. J. Bacteriol.* **170,** 5018–5026 (1988).

7. Leonhardt, K. & Strauss, N. An iron stress operon involved in photosynthetic electron transport in the marine cyanobacterium *Synechococcus* sp. PCC 7002. *J. Gen. Microbiol.* **138,** 1613–1621 (1992).
8. Zouni, A. *et al.* Crystal structure of photosystem II from *Synechococcus elongatus* at 3.8 Å resolution. *Nature* **409,** 739–743 (2001).
9. Pakrasi, H. B., Riethman, H. C. & Sherman, L. A. Organization of pigment proteins in the photosystem II complex of the cyanobacterium *Anacystis nidulans* R2. *Proc. Natl Acad. Sci. USA* **82,** 6903–6907 (1985).
10. Park, Y.-I., Sandström, S., Gustafsson, P. & Öquist, G. Expression of the IsiA gene is essential for the survival of the cyanobacterium *Synechococcus* sp. PCC 7942 by protecting photosystem II from excess light under iron limitation. *Mol. Microbiol.* **32,** 123–129 (1999).
11. Jordan, P. *et al.* Three-dimensional structure of cyanobacterial photosystem I at 2.5 Å resolution. *Nature* **411,** 909–917 (2001).
12. Boekema, E. J. *et al.* Green plant photosystem I binds light-harvesting complex I on one side of the complex. *Biochemistry* **40,** 1029–1036 (2001).
13. Lelong, C. *et al.* Characterization of a redox active cross-linked complex between cyanobacterial photosystem I and soluble ferredoxin. *EMBO J.* **15,** 2160–2168 (1996).
14. Dekker, J. P., Boekema, E. J., Witt, H. T. & Rögner, M. Refined purification and further characterization of oxygen-evolving and Tris-treated photosystem II particles from the thermophilic cyanobacterium *Synechococcus* sp. *Biochim. Biophys. Acta* **936,** 307–318 (1988).
15. La Roche, J. *et al.* Independent evolution of the prochlorophyte and green plant chlorophyll a/b light-harvesting proteins. *Proc. Natl Acad. Sci. USA* **93,** 15244–15248 (1996).
16. Garczarek, L., Hess, W., Holtzendorff, J., van der Staay, G. & Partensky, F. Multiplication of antenna genes as a major adaptation to low light in a marine prokaryote. *Proc. Natl Acad. Sci. USA* **97,** 4098–4101 (2000).
17. Boekema, E. J. *et al.* Supramolecular organization of the photosystem II complex from green plants and cyanobacteria. *Proc. Natl Acad. Sci. USA* **92,** 175–179 (1995).
18. Karrasch, S., Bullough, P. & Ghosh, R. The 8.5 Å projection map of the light-harvesting complex I from *Rhodospirillum rubrum* revelas a ring composed of 16 subunits. *EMBO J.* **14,** 631–638 (1995).
19. McDermott, G. *et al.* Crystal structure of an integral membrane light-harvesting complex from photosynthetic bacteria. *Nature* **374,** 517–521 (1995).
20. Exss-Sonne, P., Toelle, J., Bader, K., Pistorius, E. & Michel, K.-P. The IdiA protein of *Synechococcus* sp. PCC 7942 functions in protecting the acceptor side of photosystem II under oxidative stress. *Photosynth. Res.* **63,** 145–157 (2000).
21. Wenk, S.-O. & Kruip, J. Novel, rapid purification of the membrane protein photosystem I by high-performance liquid chromatography on porous materials. *J. Chromatogr. B* **737,** 131–142 (2000).
22. Van Heel, M. & Frank, J. Use of multivariate statistics in analysing the images of biological macromolecules. *Ultramicroscopy* **6,** 187–194 (1981).
23. Harauz, G., Boekema, E. & van Heel, M. Statistical image analysis of electron micrographs of ribosomal subunits. *Methods Enzymol.* **164,** 35–49 (1988).
24. Hiyama, T. & Ke, B. Difference spectra and excitation coefficients of P700. *Biochim. Biophys. Acta* **267,** 160–171 (1972).

Acknowledgements

We thank A. Kühl and F. Pfeil for technical assistance, and our colleagues M. Rögner and A. Trebst for discussions. Financial support of the Deutsche Forschungsgemeinschaft (J.K. and E.K.P.), Nederlandse Organisatie voor Wetenschappelijk Onderzoek (E.J.B.) and the Fonds der chemischen Industrie (J.K.) is gratefully acknowledged.

Correspondence and requests for materials should be addressed to E.K.P. (e-mail: e.pistorius@biologie.uni-bielefeld.de) or J.K. (e-mail: jochen.kruip@ruhr-uni-bochum.de).

erratum

Elevated c-*myc* expression facilitates the replication of SV40 DNA in human lymphoma cells

Marie Classon, Marie Henriksson, Janos Sümegi, George Klein & Marie-Louise Hammarskjöld

Nature **330,** 272–274 (1987).

In this Letter, the last name of Marie-Louise Hammarskjöld was misspelled as 'Hammaskjöld'. □